added. Five volumes of a 10% suspension of Protein A–Sepharose in RIPA was added, and this mixture was incubated with continuous gentle agitation overnight. The pellet was washed four times with 1 ml of RIPA and transferred to a fresh tube on the final wash. The resultant pellet was resuspended in (×1) SDS sample buffer, and the proteins were analyzed by SDS–polyacrylamide gel electrophoresis (SDS-PAGE) and autoradiography.
21. Full-length human c-Jun protein was produced from mRNA synthesized in vitro with a T7 expression vector that contained the coding region of human c-Jun.
22. For interaction cloning, recombinant λgt11 bacteriophage were plated and induced with IPTG (*34*). Nitrocellulose filters were processed through a denaturation-renaturation cycle as described (*35*). After renaturation, filters were incubated for 60 min in ×1 Hepes binding buffer (HBB) with 1 mM DTT, 5% Carnation nonfat powdered milk (milk), and 0.05% Nonidet P-40 (NP-40), followed by incubation for 30 min in ×1 HBB with 1 mM DTT, 1% milk, and 0.05% NP-40. Hybridization solution [Hyb(75)] consisted of 20 mM Hepes-KOH (pH 7.7), 75 mM KCl, 0.1 mM EDTA, 2.5 mM $MgCl_2$, 1% milk, 1 mM DTT, and 0.05% NP-40, to which was added HMK-phosphorylated probe protein to a final concentration of between 1×10^5 and 3.5×10^5 cpm per milliliter. After hybridization (~12 to 16 hours), filters were washed in three changes of Hyb(75) (without probe) for a total elapsed wash time not exceeding 30 min.
23. The HeLa cell library was derived from polyadenylated mRNA isolated from HeLa cells that had been treated with human γ-interferon (Immuneron, Biogen) for 48 hours. A random-primed, size-selected (>500 bp) cDNA library was prepared in λgt11 by Stratagene. The primary library size was 7×10^6 recombinants. Clones (1×10^6) from the primary library were amplified, which yielded a titer of $\sim 5.5 \times 10^{10}$ plaque-forming units per milliliter. The amplified library was used in all subsequent manipulations.
24. N. Nomura *et al.*, *Nucleic Acids Res.* **18**, 3047 (1990).
25. The cDNA insert that encoded FIP was subcloned into the Eco RI site of pBluescript (KS^+), and a nested series of deletions was generated (Erase-a-Base System, Promega). This partial cDNA clone was predicted to encode the FIP polypeptide as shown (Fig. 2B). DNA sequences of purified clones were determined on an Applied Biosystems 373 A DNA sequencer.
26. R. W. Carthew, L. A. Chodosh, P. A. Sharp, *Genes Dev.* **1**, 973 (1987); L. A. Chodosh, R. W. Carthew, J. G. Morgan, G. R. Crabtree, P. A. Sharp, *Science* **238**, 684 (1987); L. N. Peritz *et al.*, *J. Biol. Chem.* **263**, 5005 (1988); K. W. Scotto, H. Kaulen, R. G. Roeder, *Genes Dev.* **3**, 651 (1989).
27. M. Sawadogo and R. G. Roeder, *Cell* **43**, 165 (1985); R. W. Carthew, L. A. Chodosh, P. A. Sharp, *ibid.*, p. 439; N. G. Miyamoto, V. Moncollin, J. M. Egly, P. Chambon, *EMBO J.* 4, 3563 (1985).
28. An 879-bp DNA insert that encoded FIP was subcloned into a T7 promoter-directed expression vector. The plasmid was linearized by digestion with Not I and used for in vitro production of mRNA. For production of FIP(ΔZip), the plasmid vector was linearized by digestion with Sst I. For electrophoretic mobility-shift assays (*29*), reactions contained 10 mM Hepes-KOH (pH 7.8), 75 mM KCl, 2.5 mM $MgCl_2$, 0.1 mM EDTA, 1 mM DTT, 3% Ficoll 400, 0.5% polyvinyl alcohol, poly(dI-dC) · poly(dI-dC) (0.8 μg per microliter of solution), and ~0.1 ng of labeled oligonucleotide probe that contained AMLP-USE. The sequences of the probe and the competitor DNAs were: AMLP-USE, 5′-GATCCTAGGCCACGTGACCGG; μE_3, 5′-GATCCAGGTCATGTGGCAAGG; NIR-mutant, 5′-GATCCTAGGACTCGTTAGAGG; μE_4, 5′-GATCCTACCCAGGTGGTGTTG (and their complements).
29. M. S. German, M. A. Blanar, C. Nelson, L. G. Moss, W. J. Rutter, *Mol. Endocrinol.* **5**, 292 (1991).
30. Proteins were mixed and incubated at room temperature for approximately 30 min in a reaction mixture that contained 20 mM Hepes-KOH (pH 7.7), 0.2 mM EDTA, 10% glycerol, 100 mM KCl, and 1 mM DTT (HEGKD). This mixture was then diluted 10-fold with ice-cold HEGKD supplemented with 2.5 mM $MgCl_2$ and 0.1% NP-40 (HEGKMND). All subsequent steps were done at 4°C. Protein G-PLUS agarose (Oncogene Sciences) was added, and the mixture was incubated for 30 min with gentle agitation. The supernatant solution was then transferred to a fresh tube, and anti-FLAG monoclonal antibody M2 (IBI/Kodak, New Haven, CT), together with a fresh aliquot of protein G-PLUS agarose, was added. After incubation, the pellet was washed four times with HEGKMND and transferred to a fresh tube on the final wash. The washed pellet was resuspended in (×1) SDS sample buffer, and the proteins were analyzed by SDS-PAGE and fluorography (EN^3HANCE, Du Pont Biotechnology Systems).
31. P. Angel, T. Smeal, J. Meek, M. Karin, *New Biol.* **1**, 35 (1989); U. Ruther, E. F. Wagner, R. Müller, *EMBO J.* 4, 1775 (1985); R. Müller and E. F. Wagner, *Nature* **311**, 438 (1984).
32. M. I. Diamond, J. N. Miner, S. K. Yoshinaga, K. R. Yamamoto, *Science* **249**, 1266 (1990).
33. F. W. Studier, A. H. Rosenberg, J. J. Dunn, J. W. Dubendorff, *Methods Enzymol.* **185**, 60 (1990); A. H. Rosenberg *et al.*, *Gene* **56**, 125 (1987).
34. T. V. Huynh, R. A. Young, R. W. Davis, in *DNA Cloning: A Practical Approach*, D. M. Glover, Ed. (IRL Press, Oxford, 1985), vol. 1, pp. 49–78; R. A. Young and R. W. Davis, *Science* **222**, 778 (1983).
35. C. R. Vinson, K. L. LaMarco, P. F. Johnson, W. H. Landschulz, S. L. McKnight, *Genes Dev.* **2**, 801 (1988).
36. Abbreviations for the amino acid residues are: A, Ala; C, Cys; D, Asp; E, Glu; F, Phe; G, Gly; H, His; I, Ile; K, Lys; L, Leu; M, Met; N, Asn; P, Pro; Q, Gln; R, Arg; S, Ser; T, Thr; V, Val; W, Trp; and Y, Tyr.
37. F. L. Graham and A. J. van der Eb, *Virology* **52**, 456 (1973)
38. M. J. Sleigh, *Anal. Biochem.* **156**, 251 (1986).
39. G. W. Stuart, P. F. Searle, H. Y. Chen, R. L. Brinster, R. D. Palmiter, *Proc. Natl. Acad. Sci. U.S.A.* **81**, 7318 (1984).
40. We thank J. Miner for numerous reagents, protocols, and discussions; R. Turner for a human c-Jun plasmid and c-Jun antibodies; J. Johnson for a rat c-Fos plasmid; M. Leahy and Immunex Corporation for anti-FLAG M5 antibody; M. German for pBAT9; B. Chadwick for DNA sequencing; O. Venekei for oligonucleotide synthesis; and I. Herskowitz, R. Grosschedl, D. Hanahan, J. Miner, C. Peterson, and K. LeClair for critical review of the manuscript. The DNA sequence has been assigned GenBank accession number M77476. Supported by NIH grants DK-21344 and DK-41822 (W.J.R.) and by a Juvenile Diabetes Foundation International fellowship (M.A.B.).

26 December 1991; accepted 26 March 1992

Fast Perceptual Learning in Visual Hyperacuity

Tomaso Poggio, Manfred Fahle, Shimon Edelman

In many different spatial discrimination tasks, such as in determining the sign of the offset in a vernier stimulus, the human visual system exhibits hyperacuity by evaluating spatial relations with the precision of a fraction of a photoreceptor's diameter. It is proposed that this impressive performance depends in part on a fast learning process that uses relatively few examples and that occurs at an early processing stage in the visual pathway. This hypothesis is given support by the demonstration that it is possible to synthesize, from a small number of examples of a given task, a simple network that attains the required performance level. Psychophysical experiments agree with some of the key predictions of the model. In particular, fast stimulus-specific learning is found to take place in the human visual system, and this learning does not transfer between two slightly different hyperacuity tasks.

For any given visual task, it is tempting to propose a specific algorithm and a corresponding neural circuitry. It has been often implicitly assumed that this machinery may be hardwired in the brain. This extreme point of view, if taken seriously, may quickly lead to absurd consequences. Consider for instance the many different hyperacuity tasks (*1*), some of which are shown in Fig. 1. Computational analysis reveals that the photoreceptor spacing and the low-pass characteristics of the eye's optics satisfy (in the fovea) the constraints of the sampling theorem (*2*). Thus, the underlying reason for the spectacular performance of human subjects in hyperacuity tasks is that the signal sampled by the photoreceptors and relayed to the brain contains the information necessary for precise localization of image features. This observation, however, does not constitute an explanation of hyperacuity, because each task is different and, in principle, would require a different circuit for its solution. Note that the idea of a fine-grid reconstruction of the image in some layer of the cortex (*2*) does not address the problem, because it still requires yet another mechanism that looks at the reconstructed image and applies a different routine or circuitry for each specific hyperacuity task.

We have proposed instead (*3*) that the brain may be able to set up—possibly in the cortex—appropriate task-specific modules that receive input from retinotopic cells and learn to solve the task after a short training phase in which they are exposed to

T. Poggio, Artificial Intelligence Laboratory, Center for Biological Information Processing, Massachusetts Institute of Technology, Cambridge, MA 02139.
M. Fahle, Department of Neuroophthalmology, University Eye Clinic, D7400 Tübingen, Germany.
S. Edelman, Department of Applied Mathematics and Computer Science, The Weizmann Institute of Science, Rehovot 76100, Israel.

examples of the task. To show the plausibility of our argument, we first describe a model that learns to solve vernier acuity tasks from a few examples. Synthesizing a module from examples for a specific computational task may be often regarded as approximating a multivariate function from sparse data. We have chosen to use for function approximation the HyperBF network technique (*4*). Other schemes, such as the popular multilayer perceptrons or more traditional classification techniques (*5*), could probably be used as well. In our model we take the extreme view that the inputs are photoreceptor activities to demonstrate the plausibility of low-level, or "early," learning. Biologically, it may be more reasonable to assume that the input to the learning stage is provided by the circular center-surround and oriented cells in V1 (*6*, *7*).

In the simulated experiments, the learning module was given an array of "photoreceptor" cell activities that corresponded to the input image blurred by the eye's optics. There were eight "receptors," positioned randomly (Fig. 2). Each of the inputs was calculated by integrating the image over the point-spread function of the optics, approximated by a Gaussian of spatial extent σ = 30 arc sec. The simulated "retinal" patch had spatial dimensions of 180 by 360 arc sec. The eight-component vector of receptor outputs constituted the input to the HyperBF module, which was trained to produce an output of +1 for one sense of the input vernier displacement and −1 for the other over a set of examples of verniers randomly placed relative to the photoreceptor array (*8*). A measure of performance that we have considered is the percentage of correct responses (that is, responses in which the sign of the module's output agreed with the sign of the vernier displacement, as defined during training) (*6*, *8*).

The HyperBF module learned to solve the vernier task at a hyperacuity level from a few examples (*9*). The time course of the learning (Fig. 3A) shows that the output classification error rate came within 10% of its asymptotic value after ~200 examples, starting from chance-level performance at the given offset (*10*). The model replicated (*6*, *8*) several findings in the psychophysics of spatial acuity: (i) hyperacuity-level performance; (ii) improvement in the threshold with increasing length of the two segments constituting the vernier stimulus (*1*); (iii) deterioration of performance with increasing orientation difference between training and testing trials (*11*); (iv) high performance for moving verniers (*1*); and (v) performance at a similar level for another hyperacuity task, the three-point bisection, after learning from suitable examples (*12*).

The model's success demonstrates the plausibility of the hypothesis that learning of hyperacuity tasks takes place early in the visual pathway. As it stands, the model can predict the precise time course and extent of learning only if constraints are imposed on some of the parameters. Nevertheless, even in the absence of such constraints, a critical test is provided by the predictions that learning of a hyperacuity task should be fast and may not transfer even to a slightly different hyperacuity task. The HyperBF model indeed learns quickly, and it exhibits no transfer of learning between vertical and horizontal verniers (Fig. 3, A and B) (*6*). We set out to verify experimentally these predictions for human hyperacuity performance. The results of the psychophysical experiments have borne out the predictions of the model. First, the vernier threshold and the error rate in naïve subjects improved quickly over a few tens of trials (Fig. 4A). Second, the subjects exhibited no transfer of learning between the vertical vernier and the horizontal vernier tasks or vice versa (Fig. 4B). In additional experiments, there was no significant interocular transfer of learning and no transfer between line and dot (Fig. 1) stimuli (*13*). The experiments, as well as the simulations, involved learning with feedback. Preliminary experiments show that human subjects can learn even in the absence of feedback, but more slowly. The algorithm we used in our simulations can also be made to learn the hyperacuity task in the absence of feedback, at a slower rate (*6*, *7*).

Our findings on fast stimulus-specific learning suggest that the effect shown in Fig. 4A cannot be due solely to a simple adaptive process, such as a change in the overall detection threshold. In that, our results are similar to other known instances of perceptual learning. A prominent example is provided by the work of Fiorentini and Berardi (*14*), who demonstrated stimulus-specific learning effects in the discrimination of mixed spatial frequency gratings that suggested the involvement of an early-stage mechanism. In results similar to ours, they found that learning did not transfer between different orientations of the grating. They also found that there was interocular transfer of learning but little transfer across retinal locations. Karni and Sagi (*15*) recently described a texture discrimination task in which the subjects showed a (much slower) stimulus-specific learning effect that did show interocular transfer but did not transfer either across orientations or across positions. Other similar instances of specific perceptual learning had been reported even earlier (*16*), and even in hyperactivity, though on a much slower time scale, by McKee and Westheimer [in (*16*)]. Plasticity early in the visual pathway has been demonstrated experimentally (*17*) and could provide the adaptive mechanisms required by a module of the HyperBF type.

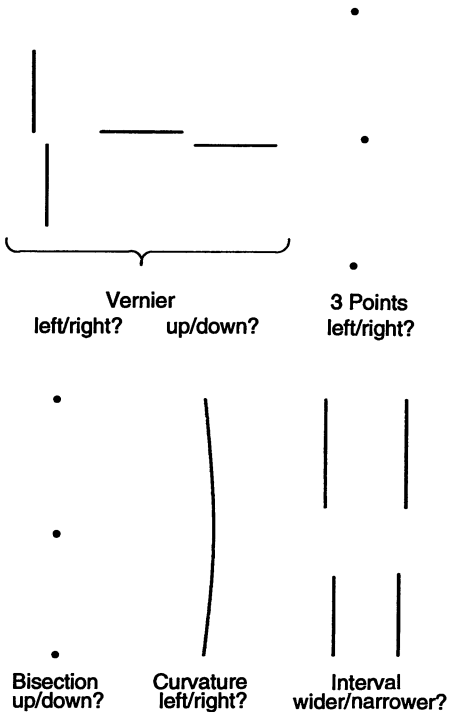

Fig. 1. Examples of five tasks in which human subjects perform at hyperacuity levels (that is, exhibit resolution finer than the spacing between individual photoreceptors).

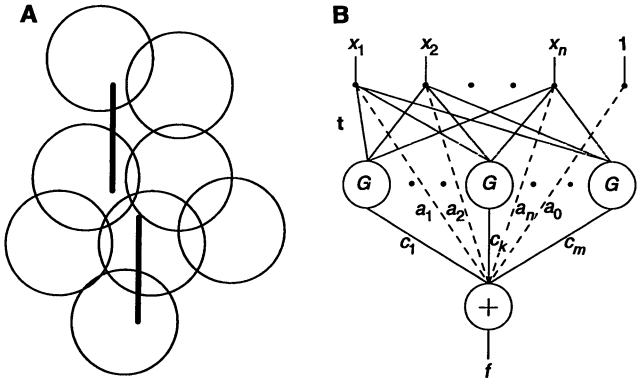

Fig. 2. (**A**) A vernier stimulus, superimposed on the mosaic of receptive fields of "cells" assumed to provide the input to the HyperBF module shown in (B). Each receptive field is depicted as a circle that refers to the point-spread function of the optics. Our simulation is robust with respect to positioning the "cells" at precisely defined locations and with respect to their receptive field properties. (**B**) A network equivalent to Eq. 1 (*4*).

Our computational and psychophysical results support the conjecture that the modules responsible for hyperacuity-level performance are synthesized or improved early in the visual pathway in a demand-driven fashion when the appropriate task is first performed by the subject. Related evidence regarding perceptual learning mentioned above suggests that the same line of reasoning can be applied to visual tasks other than hyperacuity, and even to faculties other than vision (*3*, *18*). Importantly, a learning HyperBF interpolation can be implemented in a simple, biologically plausible network (*3*, *4*). The proposal that much of the information processing in the brain is performed by mechanisms related to the HyperBF modules acting as enhanced look-up tables may bridge apparently conflicting paradigms, such as Gibson's immediate perception and Marr's representational theory, because appropriately encoded icons or "snapshots" of the world appear to allow the synthesis of computational mechanisms effectively equivalent to vision algorithms for tasks ranging from hyperacuity to object recognition (*19*).

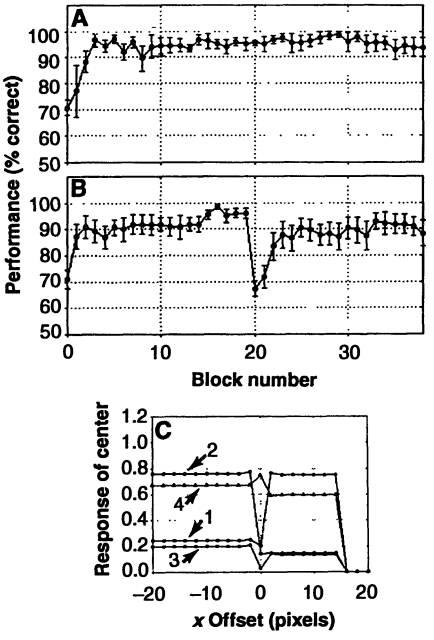

Fig. 3. (**A**) Time course of learning by a HyperBF module given the input shown in Fig. 2A (vertical verniers appearing at random positions, with random offsets uniformly distributed between 12 and 18 arc sec of visual angle). Each block in this simulation consisted of 40 trials; the ordinate shows the percentage of correct responses in each block (mean ± 1 standard error over six simulation runs). (**B**) Effect of changing stimulus orientation at block 20 (means of 12 runs; in 6 runs the change was from vertical to horizontal, and in another 6 runs the change was from horizontal to vertical). There was no transfer of learning, as expected, because the examples used by the network corresponded to very different patterns of activation of the inputs in the two cases. Feedback was provided in these simulations (but is not strictly required by the learning algorithm). (**C**) Responses of the four HyperBF centers (acquired during an incremental learning session that consisted of 150 trials) versus the offset of a vertical vernier presented at a fixed location. During learning, the offsets were uniformly distributed between 8 and 12 pixels. The response was tested with vertical verniers shown at the same location, with an offset ranging from −20 to 20 pixels. This illustration may be regarded as a recording of the receptive fields of the centers in the space of possible inputs. Of the four centers, one responded strongly to positive offsets and weakly to negative ones, another preferred negative offsets, and the other two had no clear preference for any offset sign. An appropriate response representing the sign of the offset may be formed at the output level of the HyperBF module with the responses of the sign-selective centers.

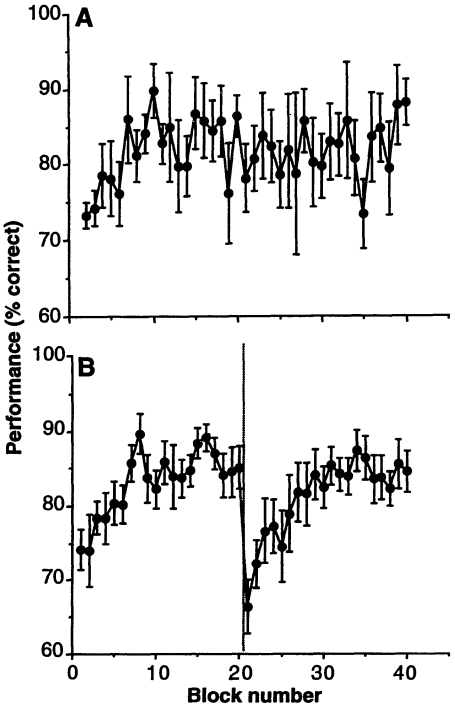

Fig. 4. Psychophysical experiments corresponding to the simulations of Fig. 3. (**A**) Time course of learning in a vernier task. Verniers were 20 arc min long and 2 arc min wide, presented on a cathode-ray tube screen with >95% contrast under photopic conditions at a viewing distance of 2.5 m with a constant offset (between 15 and 20 arc sec, depending on the subject). Percentages of correct responses in a 2AFC task improved rapidly during the initial period of learning, that is, during about 100 presentations. Data are means of six naïve observers; vertical bars represent standard errors. Each block consisted of 40 trials. We found similar learning effects with verniers consisting of three dots rather than two lines. The percentage of correct responses was chosen to represent learning instead of the more usual threshold because the time resolution of the latter measure is too poor compared with the time scale of the learning effects. (**B**) Effect of switching from vertical to horizontal verniers (or vice versa) after block 20. Averaged results of 12 naïve subjects; 6 started with horizontal verniers, and the others started with vertical verniers. There is no transfer of learning. In these experiments, feedback was provided to the subjects [other experiments, reported in (*10*), showed that learning also occurred in the absence of feedback].

REFERENCES AND NOTES

1. G. Westheimer and S. P. McKee, *Vision Res.* **17**, 941 (1977).
2. F. H. C. Crick, D. C. Marr, T. Poggio, in *The Organization of the Cerebral Cortex*, F. Schmitt, Ed. (MIT Press, Cambridge, MA, 1980), pp. 505–533; H. B. Barlow, *Nature* **279**, 189 (1979). The sampling theorem states that a signal that contains no frequency components for $|f| \geq W$ is completely described by its samples, uniformly spaced with period $T_s \leq 1/2W$ [for example, H. S. Black, *Modulation Theory* (Van Nostrand, Princeton, NJ, 1953)].
3. T. Poggio, in *Cold Spring Harbor Symp. Quant. Biol.* **LV**, 899 (1990).
4. _____ and F. Girosi, *A.I. Memo No. 1140* (Artificial Intelligence Laboratory, Massachusetts Institute of Technology, Cambridge, MA, 1989); *Proc. IEEE* **78**, 1481 (1990). The HyperBF network scheme for the approximation of smooth functions has the form

$$f^*(\mathbf{x}) = \sum_{\alpha=1}^{m} c_\alpha G(\|\mathbf{x} - \mathbf{t}_\alpha\|^2_{\mathbf{W}}) + p(\mathbf{x}) \qquad (1)$$

where the parameters $\mathbf{t}_\alpha$ that correspond to the centers of appropriate basis functions G (such as the Gaussian) and the coefficients c_α are unknown and are in general much fewer than the data points ($m \leq N$). The norm is a weighted norm

$$\|\mathbf{x} - \mathbf{t}_\alpha\|^2_{\mathbf{W}} = (\mathbf{x} - \mathbf{t}_\alpha)^T\mathbf{W}^T\mathbf{W}(\mathbf{x} - \mathbf{t}_\alpha) \qquad (2)$$

where $\mathbf{W}$ is an unknown square matrix and the superscript T indicates the transpose.

The network of Fig. 2B corresponds exactly to Eq. 1. Its interpretation is as follows. The centers of the basis functions are similar to prototypes (see Fig. 3C) because they are points in the multidimensional input space. Each unit computes a (weighted) distance of the inputs from its center and applies to it the radial function. In the case of the Gaussian, a unit will be the most active when the input exactly matches its center. The output of the network is a linear superposition of the activities of all of the basis functions, plus direct, weighted connections from the inputs [the linear terms of $p(\mathbf{x})$] and from a constant input (the constant term). In the limit case of the basis functions approximating delta functions, the system becomes equivalent to a look-up table holding the examples.

The parameters $\mathbf{c}$, $\mathbf{t}$, and $\mathbf{W}$ are searched for during learning by minimizing an error functional defined as

$$H[f^*] = H_{\mathbf{c},\mathbf{t},\mathbf{W}} = \sum_{i=1}^{N} (\Delta_i)^2$$

where

$$\Delta_i \equiv y_i - f^*(\mathbf{x})$$

$$= y_i - \sum_{\alpha=1}^{m} c_\alpha G(\|\mathbf{x}_i - \mathbf{t}_\alpha\|^2_{\mathbf{W}})$$

and y_i are the desired outputs. Thus, learning in the HyperBF network corresponds to finding values of parameters that minimize H. Iterative methods of the gradient descent type can be used for the minimization of H. An even simpler method

that does not require calculation of derivatives is to look for random changes (controlled in appropriate ways) in the parameter values that reduce the error. In the simulations described in this report the model was endowed with a dual, incremental learning mechanism. First, when the model's performance on a new input was markedly inadequate (in comparison with recent history), that input was adjoined to the model as an additional center (prototype). This happened mainly in the initial trials, with the number of centers eventually reaching an asymptote that depended on the nature of the task and on the parameters that affected the decision to add new centers. The performance of the model during these first trials improved quickly, then stabilized as the number of centers approached the asymptote. Second, further gradual improvement in the performance was obtained by letting the model carry out a local random search in the space of existing HyperBF center coordinates. This search was guided by feedback given to the model (that is, by indicating whether the response at each trial was correct). Details of the learning algorithms, including an extension of the incremental learning algorithm to a situation in which no explicit feedback is available, can be found in (*6, 7*).

5. A description of multilayer perceptrons and the back-propagation technique used for learning is in D. E. Rumelhart, G. E. Hinton, R. J. Williams, *Nature* **323**, 533 (1986). An overview of some of the classical techniques can be found in S. Omohundro [*Complex Syst.* 1, 273 (1987)] and in R. O. Duda and P. E. Hart [*Pattern Classification and Scene Analysis* (Wiley, New York, 1973)]. Relations between multilayer perceptrons and HyperBF networks are mentioned in (*4*) and studied in M. Maruyama, F. Girosi, T. Poggio, *A.I. Memo No. 1291* (Artificial Intelligence Laboratory, Massachusetts Institute of Technology, Cambridge, MA, 1992).
6. T. Poggio, M. Fahle, S. Edelman, *A.I. Memo No. 1271* (Artificial Intelligence Laboratory, Massachusetts Institute of Technology, Cambridge, MA, 1991); S. Edelman, T. Poggio, M. Fahle, *Comput. Vision Graph. Image Process.* B, in press. The simulation results were robust with respect to all parameters, including the number of inputs.
7. Y. Weiss, S. Edelman, M. Fahle, T. Poggio, *CS-TR 91-21* (Department of Applied Mathematics and Computer Science, Weizmann Institute, Rehovot, Israel, 1991).
8. We have also experimented with a different version of the HyperBF model, in which orientation-selective receptive fields similar to those of simple cells in V1 played the role of the basis functions. See (*7*). This version of the model replicated the absolute values and the time course of the improvement of the thresholds found in human psychophysical data, in addition to replicating the data concerning the percentage of correct responses.
9. Hyperacuity-level performance was independent of the precise location of the receptors. At the same time, different quasi-random receptor mosaics yielded different thresholds, sometimes by as much as a factor of 2. A similar range of hyperacuity thresholds is observed in human subjects, even at full acuity and with perfectly normal eyes.
10. The model also exhibited learning on a longer time scale (*4, 7*), similar to the slow long-term learning component found in human subjects (M. Fahle and S. Edelman, in preparation).
11. R. Watt and F. W. Campbell, *Spat. Vision* 1, 31 (1985).
12. The stimulus in the bisection task consists of three dots, arranged in a vertical line, at an approximately even spacing. The subject has to determine whether the middle dot is above or below the midpoint of the segment formed by the other two dots. The HyperBF module learned this hyperacuity task just as easily as it did in the line vernier case (*6*). Another simulation made a comparison between the line vernier task and a similar one in which each of the line segments has been replaced by two dots (situated at the endpoints). The network learned this task, as it did previously in the line vernier and the bisection cases. The better performance of the HyperBF module in the dot vernier task for small offsets parallels a recent surprising finding with human subjects (M. Fahle, unpublished observations).
13. In a recent study, R. Bennett and G. Westheimer [*Percept. Psychophys.* **49**, 541 (1991)] found surprisingly little learning of thresholds in three-dot alignment and grating discrimination. Their experiments used transfer of training across the stimulus range to probe for learning, hiding possible effects of fast learning that may have happened in the baseline session (p. 544). Interestingly, the lack of transfer across the stimulus range in these experiments is consistent with our notion of experience-based learning.
14. A. Fiorentini and N. Berardi, *Nature* **287**, 43 (1980).
15. A. Karni and D. Sagi, *Proc. Natl. Acad. Sci. U.S.A.* **88**, 4966 (1991).
16. K. Ball and R. Sekuler, *Science* **218**, 697 (1982); S. P. McKee and G. Westheimer, *Percept. Psychophys.* **24**, 258 (1978); V. S. Ramachandran and O. Braddick, *Perception* **2**, 371 (1973).
17. Y. Frégnac, D. Shulz, S. Thorpe, E. Bienenstock, *Nature* **333**, 367 (1988).
18. T. Poggio and S. Edelman, *ibid.* **343**, 263 (1990); S. Edelman and T. Poggio, *Int. J. Pattern Recognit. Artif. Intell.*, in press; S. Edelman and D. Weinshall, *Biol. Cybern.* **64**, 209 (1991).
19. S. Edelman, D. Reisfeld, Y. Yeshurun, *CS-TR 91-20* (Department of Applied Mathematics and Computer Science, Weizmann Institute, Rehovot, Israel, 1991); R. Brunelli and T. Poggio, in *Proceedings of the 12th International Joint Conference on Artificial Intelligence*, International Joint Conference on Artificial Intelligence, Inc., Sydney, Australia, 24 to 30 August 1991 (Kaufmann, Mountain View, CA, 1991); S. Edelman and T. Poggio, *A.I. Memo No. 1181* (Artificial Intelligence Laboratory, Massachusetts Institute of Technology, Cambridge, MA, 1990); R. Brunelli and T. Poggio, *I.R.S.T. TechReport 9110-04* (Instituto per la Ricerca Scientifica e Tecnologica, Trento, Italy, 1991).
20. We are grateful to H. Buelthoff, F. Crick, F. Girosi, R. Held, A. Hurlbert, Y. Weiss, and G. Westheimer for useful discussions and suggestions. Supported by a grant from the Office of Naval Research, Cognitive and Neural Sciences Division, by the Artificial Intelligence Center of Hughes Aircraft Corporation, and by the Deutsche Forschungsgemeinschaft (Heisenberg-Programme). Support for the Artificial Intelligence Laboratory's artificial intelligence research is provided by the Advanced Research Projects Agency of the Department of Defense. T.P. is supported by the Uncas and Helen Whitaker chair.

18 December 1991; accepted 24 March 1991

Synaptotagmin: A Calcium Sensor on the Synaptic Vesicle Surface

Nils Brose,* Alexander G. Petrenko, Thomas C. Südhof, Reinhard Jahn†‡

Neurons release neurotransmitters by calcium-dependent exocytosis of synaptic vesicles. However, the molecular steps transducing the calcium signal into membrane fusion are still an enigma. It is reported here that synaptotagmin, a highly conserved synaptic vesicle protein, binds calcium at physiological concentrations in a complex with negatively charged phospholipids. This binding is specific for calcium and involves the cytoplasmic domain of synaptotagmin. Calcium binding is dependent on the intact oligomeric structure of synaptotagmin (it is abolished by proteclytic cleavage at a single site). These results suggest that synaptotagmin acts as a cooperative calcium receptor in exocytosis.

Calcium-dependent exocytosis of synaptic vesicles is the central step in the sequence of events from the arrival of an action potential to the release of neurotransmitters. It is generally accepted that Ca^{2+} enters the nerve terminal via voltage-gated Ca^{2+} channels in the presynaptic plasma membrane. Intracellular recordings in model synapses such as the squid giant synapse have shown that the latency between Ca^{2+} entry and the release of transmitter is in the range of 200 μs. This implies that a complex between synaptic vesicles and the plasma membrane must exist in the resting state because the time after Ca^{2+} entry is too short to allow for vesicle docking before fusion. Furthermore, the dependence of transmitter release on the intraterminal Ca^{2+} concentration is nonlinear and highly cooperative (*1*).

The Ca^{2+} receptor protein for exocytosis has not been identified. However, certain predictions about its properties can be made. Because of the short latency between Ca^{2+} influx and exocytosis, it is likely that the Ca^{2+} receptor is part of the complex formed between the plasma membrane and the synaptic vesicle and is probably located on one of these membrane compartments. In addition, Ca^{2+} must induce a change in the properties of the receptor protein, which ultimately causes a rearrangement of

N. Brose and R. Jahn, Department of Neurochemistry, Max-Planck-Institute for Psychiatry, D-8033 Martinsried, Germany.
A. G. Petrenko and T. C. Südhof, Howard Hughes Medical Institute and Department of Molecular Genetics, University of Texas Southwestern Medical Center, Dallas, TX 75235.

*Present address: Salk Institute, Molecular Neurobiology Laboratory, 10010 North Torrey Pines Road, La Jolla, CA 92037.
†Present address: Howard Hughes Medical Institute and Department of Pharmacology, Yale University School of Medicine, New Haven, CT 06536.
‡To whom correspondence should be addressed.